Free-Energy Landscapes of Proteins in the Presence and Absence of Force

Zu Thur Yew,[†] Sergei Krivov,[‡] and Emanuele Paci*,[†]

Institute of Molecular and Cellular Biology, University of Leeds, U.K., and ISIS, Université Louis Pasteur, Strasbourg, France

Received: August 15, 2008; Revised Manuscript Received: October 6, 2008

The *equilibrium* properties of the fourth immunoglobulin domain of filamin from *Dictyostelium discoideum* (ddFLN4) in the absence and presence of a small force (0−6 pN) pulling the termini apart is characterized through atomistic numerical simulation. The equilibrium free-energy landscape of ddFLN4 is found to change in a complex fashion that cannot be described in terms of one-dimensional projections as usually done in the interpretation of mechanical (un)folding experiments. Nonequilibrium unfolding simulations reveal that the major unfolding intermediate corresponds to a marginally populated state at equilibrium that only appears when a force larger than 4 pN is applied. Finally, we show that if the free-energy difference between states is taken to be linear in the applied force, the proportionality coefficient is not the difference in the end-to-end distance between pair of states as generally assumed even though the data can be reasonably fitted. The present results suggest that mechanical unfolding experiments may reveal states that are not accessible in the absence of force. Thus, special care should be taken when trying to interpret both equilibrium and nonequilibrium mechanical (un)folding experiments in light of the (un)folding properties in the absence of a force.

Introduction

Dynamic force spectroscopy techniques such as atomic force microscopy and optical tweezers have in recent years been extensively applied to study the mechanical response of biomolecules to an applied force.[1,2] With better spatial, temporal, and force resolution, dynamic force spectroscopy techniques have been increasingly utilized as a means of exploring the underlying free-energy landscape of proteins. Crucial to the ability of such techniques to accomplish such a detailed mapping is the exquisite sensitivity of these techniques to changes in the contour length of a protein upon the application of a force, which can be related to the number of residues involved in the unfolding event.[3,4] Thus, not only can distinct conformational states (e.g., (un)folding intermediates) be detected, a precise characterization of their structural properties can also be obtained when coupled with judiciously chosen mutations.[5,6] Even when mutational analysis is not possible, the distribution of forces or dwell times can give insight into the relative free-energy between two states, if the states are resolved by the force-measuring instrument,[7,8] and the global features of the underlying free-energy landscape such as its roughness and shape.[9−11]

The characterization of the (un)folding pathways and free-energy landscapes of a number of proteins have been reported and include the fourth immunoglobulin domain of filamin from *Dictyostelium discoideum*[5,6,12] (ddFLN4), GFP,[13] ubiquitin,[2,9] and RNaseH.[7] Li and co-workers[14] have recently observed two parallel pathways in the mechanical unfolding of T4 lysozyme where the minor pathway involves an unfolding intermediate. In another work, Samori and colleagues[15] reported three classes of conformational substates of monomeric alpha-synuclein and related them to its amyloidogenicity. An intriguing suggestion emerging from these studies is that the properties of proteins under mechanical load are directly related to those in the absence of force.

The manner in which the free-energy landscape of a protein is modified by the presence of a force has not been conclusively determined. In practical terms, it is not clear whether a small force merely increases the detectability of partially folded states along the (un)folding pathway ("on-pathway") at zero force, as assumed in most studies, or if the force significantly stabilize states that are otherwise not significantly populated or "off-pathway".

The effect of the applied force on the free-energy of a system is given by $G_F = G_0 - Fx$ where x is the extension (i.e., distance between the points of application of the force) of the system. The relative free-energy between two conformations with different extensions after the application of the force is then $\Delta G_F = \Delta G_0 - F\Delta x$ where Δx is the difference in extension between the two conformations. The latter equation is embedded in the phenomenological Bell model and typically used to analyze mechanical unfolding experiments. Δx, which has the dimensions of length, is often interpreted as being indicative of some molecular entity; for example, the size of a solvent molecule[16] or the amount hydrogen bonds holding a pair of β-strands must elongate to reach the transition state for unfolding.[16−18] While the free-energy between two conformations, each having a particular extension (e.g., 10 and 100 Å), is indeed linear in the applied force, the *average extension* of a particular *state* (e.g., the native state of a protein) is expected to change with the force since it is not static but dynamic. Thus, if the average extension of the two states in question do not change in the same direction, the linear dependence of ΔG_F on the applied force is unlikely to be valid.[19] Consequently, the linear coefficient, Δx, extracted from a linear fit of ΔG_F need not be the difference in extension between two states. Due to the difficulty in characterizing transition states or ground states

* To whom correspondence should be addressed. E-mail: e.paci@leeds.ac.uk.
[†] University of Leeds.
[‡] Université Louis Pasteur.

10.1021/jp807316e CCC: $40.75
Published on Web 11/18/2008

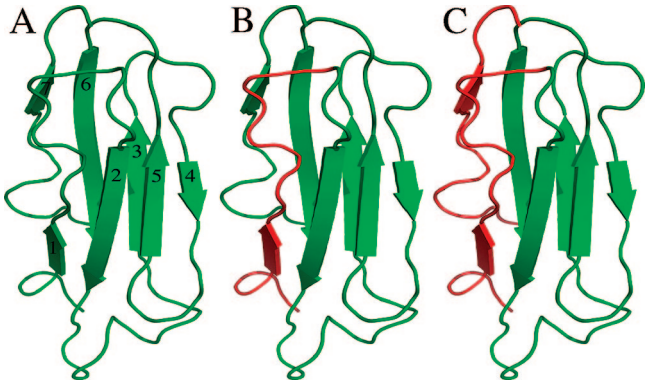

Figure 1. Structural properties of the equilibrium states. (A) NMR structure of ddFLN4 (PDB ID: 1ksr); individual strands labeled 1−7. (B) Structured core of the intermediate I1 shown in green. (C) Structured core of the intermediate I2 shown in green.

at equilibrium even in the presence of a small force however, this has not been demonstrated or thoroughly assessed.

By using molecular dynamics (MD) simulations of a coarse-grained model of the protein ddFLN4 (Figure 1a), we characterize the equilibrium properties of ddFLN4 under a range of forces (0−6 pN) and investigate, for the first time, the aforementioned issues. Our results indicate that from 2 pN onward, the free-energy landscape of ddFLN4 is qualitatively different from that at zero force. At 5−6 pN, an intermediate state that is not populated in the absence of a force, but is the major intermediate in the nonequilibrium unfolding simulations, appears. Lastly, we evaluated the differences in free-energies between pairs of states as a function of the applied force and find that even though the relationship is approximately linear, Δx is not the difference in extension between pair of states as often assumed.

Results

Equilibrium Characterization of ddFLN4. To characterize the free-energy landscape at equilibrium, we sought conditions (temperature and force) under which reversible unfolding−folding are observed on the time scale of the simulations (several microseconds). The specific heat for different forces is shown in Figure 2a. At 330 K (close to the maximum of the specific heat) and forces in the interval of 0−6 pN, the simulations reach equilibrium and multiple transitions are observed between the folded and unfolded states as evident from the timeseries of the root-mean-square deviation from the native structure (rmsd, Figure 2b).

The timeseries of the rmsd suggests the existence of three states (the denatured (∼21−60 Å), intermediate (∼12−18 Å), and native (≤6 Å) states) with well defined transitions between them, indicating that the states are well separated by significant barriers. From the perspective of the rmsd at least, the behavior of the model is consistent with experiments.[6] In comparison to the rmsd, the end-to-end distance or extension (d_{NC}) is actually a poorer reaction coordinate and only distinguishes structures that differ considerably in d_{nc} (e.g., highly compact and extended conformers), but obscures semicompact intermediate states (Figure 3). A two-dimensional potential of mean force using d_{NC} and rmsd as variables (Figure 4, bottom panel) did not give a clearer picture and actually obscured what we will show below to be the main features of the free-energy landscape.

Such low-dimensional projections of a multidimensional landscape on conventional order parameters is in general misleading and can mask the complexity of the free-energy surface.[20] As such, the analysis was supplemented by using a

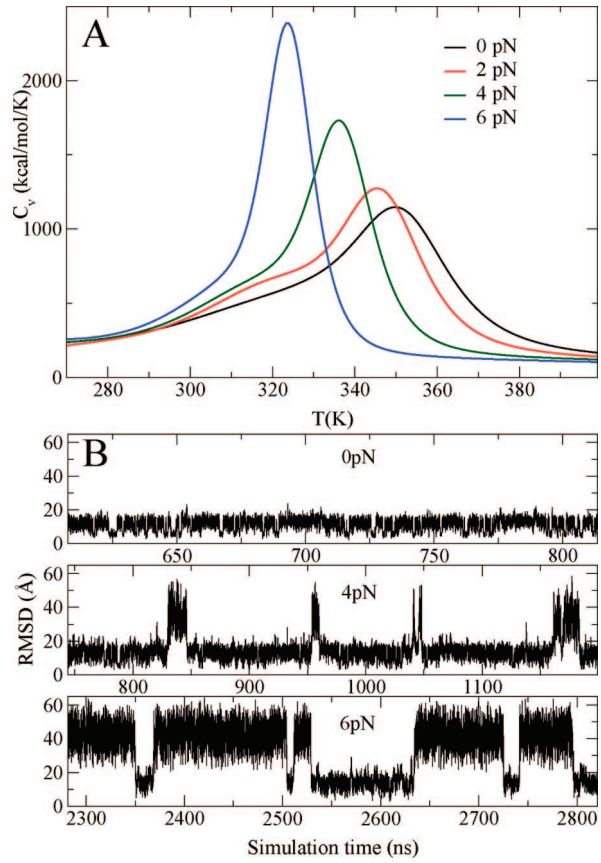

Figure 2. (A) Specific heat as a function of temperature at various forces. (B) Timeseries of the root-mean-square deviation from the native structure for the equilibrium simulations at 330 K and under a constant force of 0, 4, and 6 pN.

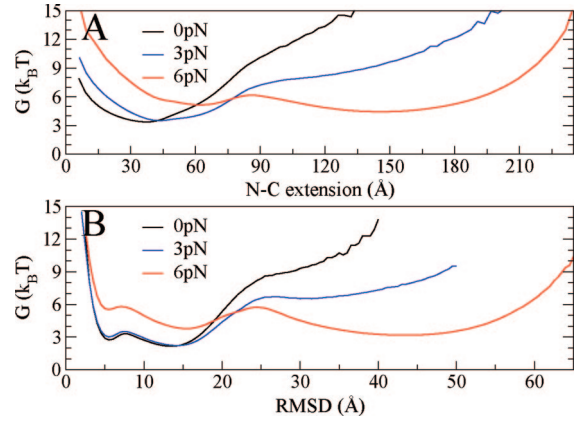

Figure 3. Conditional free-energies as a function of (A) the extension, d_{nc}, and (B) the rmsd to the native structure.

recently developed method that robustly groups the coordinate sets into free-energy minima, not according to the standard geometric characteristics, but rather the equilibrium dynamics (see Methods). The resultant free-energy profile (FEP) gives a complete description of the system kinetics[21] only when the free-energy landscape is essentially one-dimensional. If the landscape has parallel pathways, as is the case here even at small forces, these will inevitably overlap upon projection onto the one-dimensional reaction coordinate. Therefore, it is crucial to complement the analysis by using the equilibrium kinetic network (SEKN), which avoids projection and describes the kinetics in terms of direct interbasin transitions.

In contrast to the three states identified by the timeseries of the rmsd, the SEKN reveals the presence of two to four states

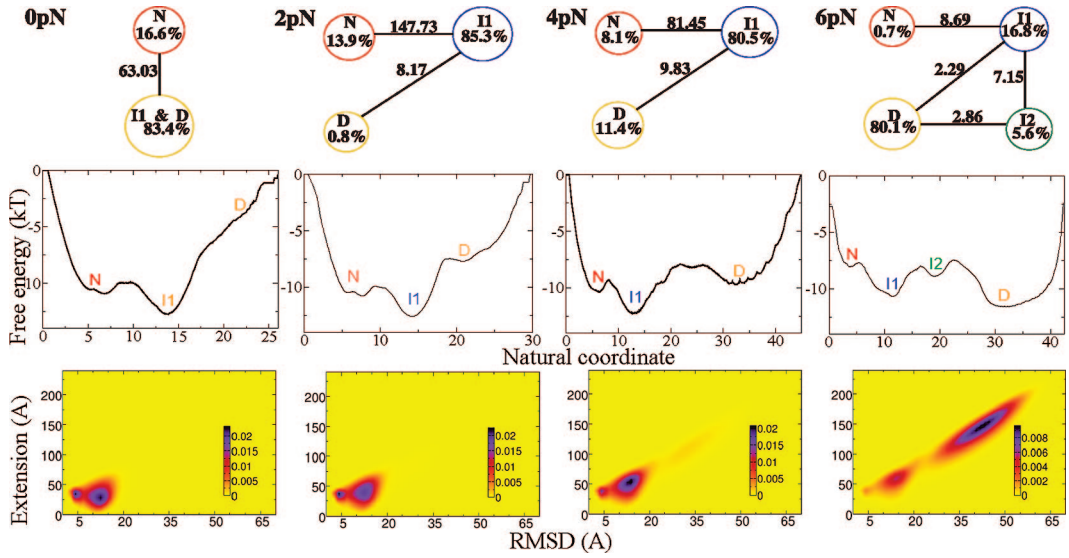

Figure 4. (top panel) SEKN for the equilibrium simulations under force. Numbers in circles denote the population of each state while those on the lines denote the rate (in inverse nanoseconds) of direct transitions between the states. (middle panel) FEP for the corresponding SEKN. (bottom panel) 2D projection of the simulations onto the rmsd and d_{NC}. The scale bar gives the frequency of each contour in the projection.

depending on the force. In Figure 4, the SEKN (top panel) and the one-dimensional FEP (middle panel) of the system along the "natural coordinate" (see Methods) at various forces and 330 K are shown.

In the absence of an applied force, there are two distinct "basins", the native, N and a second basin consisting of two distinct states, D and I1. The state I1 corresponds to a structured intermediate with strand 1 distorted (Figure 1b) while state D, which is negligibly populated (<1%), comprises of denatured conformations with relatively few native contacts (<30%). The FEP reveals that the denatured state, D, is not thermodynamically stable (i.e., its lifetime is short) and is not separated from the intermediate, I1, by a significant barrier. The protein is thus effectively two-state in the absence of a force.

When 2 pN of force is applied to the termini, the system exists in one of three states, N, I1, and D. In contrast to the situation seen in the absence of a force, states I1 and D are now distinct although the FEP suggests that D is only marginally stable. The composition of state D also becomes clearer; it is mainly made up of extended conformers where the core of the protein is largely unstructured.

At 3−4 pN of force, the denatured state, D, becomes a local minimum of the free-energy. Interestingly, at 3 pN, the denatured state D consists of two substates that are separated by a small barrier (i.e., < $1k_BT$). The first consists of semicompact conformers with varying degrees of structure; one of which, is a structured conformer corresponding to an intermediate state that becomes distinct and thermodynamically stable at higher forces (I2, see 5−6 pN below). The second substate consists of conformers that are extended and highly unstructured. At forces < 4 pN, the semicompact substate dominates, while at larger forces, only the highly extended substate is significantly populated. Thus, although there are at least two sets of denatured conformations, they are not thermodynamically distinct and can be considered as a single state that is very plastic and elongates continuously with the force. As such, while states N and I1 respond to an increase in force from 3 to 4 pN by elongating by 0.7 and 4.3 Å on average, state D elongates by 16 Å (see Table 1).

At forces of 5−6 pN, we observe a qualitative change in the free-energy landscape: a second intermediate state, I2, which consists of conformers that have strands 1 and 7 unfolded (Figure 1c), becomes stable enough to be detected. The population of I2 however, is reduced at 6 pN. This is due to the opposite effects of the force—stabilizing more extended states, but also disrupting native contacts—on semicompact yet structured states. Consistent with the observations above, there is another shift in the $\langle d_{NC} \rangle$ of all states and is particularly pronounced for state D (Table 1). At 5−6 pN of applied force, ddFLN4 is at least three-state.

TABLE 1: Average End-to-End Distances, $\langle d_{NC} \rangle$, in angstroms of the States Shown in Figure 4 at Each Force[a]

state	0 pN	1 pN	2 pN	3 pN	4 pN	5 pN	6 pN
N	35.5	36.2	37.3	38.0	38.7	39.5	39.8
I1	35.9	39.5	43.4	47.2	51.5	53.8	56.9
I2						74.3	78.5
D			87.1	91.9	107.7	126.4	142.8

[a] The $\langle d_{NC} \rangle$ computed for state D at 3 pN represents the weighted average of both the semicompact and extended substates.

Although the SEKNs at 3−4 pN and 5−6 pN are different, the overall shape of the FEP is unchanged. This highlights that even the best possible one-dimensional projection[21] may hide the inherent complexity of the landscape since they cannot represent parallel pathways. For instance at 5−6 pN, the SEKN indicates that there are two routes out of the denatured basin, D → I1 → N and D → I2 → I1 → N, and only one at 2−4 pN. The asymmetry in kinetic routes into and out of N also implies an asymmetry in the rate limiting barriers traversed. For example, the FEP indicates that there are two sizable barriers (i.e., > $1k_BT$) for the folding transition, but only one for the unfolding transition.

Nonequilibrium Mechanical Unfolding Pathways. Ten constant velocity (0.01 Å ps^{-1}) and constant force (20 pN) unfolding simulations of ddFLN4 at 330 K were analyzed to compare the states traversed in nonequilibrium unfolding pathways with those characterized at equilibrium. The unfolding intermediate, if any, was identified by visual inspection of the timeseries of native contacts between pairs of neighboring strands (Figure 5).

In both sets of simulations, the unfolding pathway can be described as: N/I1 → I2 → D (Figure 5). While I2 (Figure 1c)

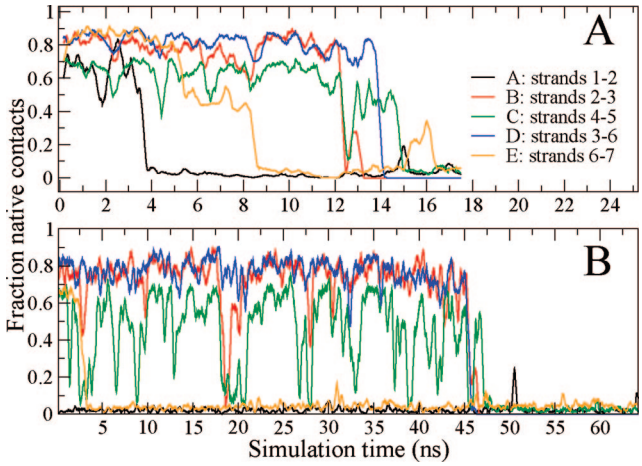

Figure 5. Timeseries of the fraction of native contacts between pairs of neighboring strands. (A) Constant velocity unfolding (0.01 Å ps^{-1}). (B) Constant force unfolding (20 pN).

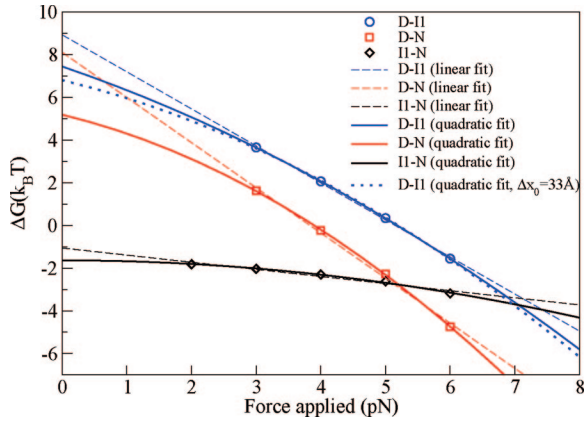

Figure 6. Plot of $\Delta G_{F,\mathrm{I1-N}}$ (black), $\Delta G_{F,\mathrm{D-N}}$ (red), and $\Delta G_{F,\mathrm{D-I1}}$ (blue) as a function of force. The dashed lines are fits to $\Delta G = \Delta G_0 - F\Delta x$. The solid lines are fits to eq 1, $\Delta G_F = \Delta G_0 - F\Delta x_0 + F^2\Delta(1/k)/2$. The parameters extracted from both fits are listed in Table 2. The relative standard deviations of the points, calculated by dividing the trajectories into two parts, are less than 9.7% except for (i) D − I1 at 4 pN (19.6%), (ii) D − I1 at 5 pN (27.2%), and (iii) D−N at 4 pN (199%).

is a major intermediate in the nonequilibrium unfolding simulations, it is a minor species at equilibrium that only becomes thermodynamically distinct when 5−6 pN of force is applied.

Free-Energy As a Function of Force. Here, we examine the assumption that the relative free-energy between states varies linearly with the force and that the linear coefficient, Δx, is the difference in $\langle d_{\mathrm{NC}}\rangle$ between two states by directly computing the difference in free-energies between pairs of states (ΔG_F in units of $k_{\mathrm{B}}T$ or $-\ln K_{\mathrm{eq}}$) as a function of the force. From Figure 6, it can be seen that ΔG_F decreases (i.e., the more extended states become favored) as the force is increased. The variation of ΔG_F is approximately linear in the small range of forces explored (i.e., $\Delta G_F = \Delta G_0 - F\Delta x$). The value of the constant Δx extracted from a linear fit (Table 2) is consistent with the overall "nativeness" of the various states (i.e., I1 is "closer" to N than D or $\Delta x_{\mathrm{D-N}} = 96.3$ Å $> \Delta x_{\mathrm{I1-N}} = 15.2$ Å). However, Δx is not the difference in $\langle d_{\mathrm{NC}}\rangle$ between pairs of states at zero force (Table 1). This highlights the inconsistency between Δx, which is independent of the force and $\langle d_{\mathrm{NC}}\rangle$, which is force dependent.

According to the analysis of Sachs and Lecar,[19] which assumes that the $\langle d_{\mathrm{NC}}\rangle$ of each state is governed by a one-dimensional harmonic potential, ΔG_F is expected to vary with the force as follows:

$$\Delta G_F = \Delta G_0 - F\Delta x_0 + F^2\Delta(1/k)/2 \qquad (1)$$

where Δx_0 is the difference in $\langle d_{\mathrm{NC}}\rangle$ between two states at zero force and $\Delta(1/k)$ is the difference in the reciprocal of the spring constants, k, between two states. Fitting the data with eq 1 not only improves upon the linear fit, but also gives estimates of Δx_0 and $\Delta(1/k)$ (Table 2) that are in reasonable agreement with those approximated from Table 1 assuming that the $\langle d_{\mathrm{NC}}\rangle$ of each state is governed by a harmonic potential characterized by a force-independent spring constant; i.e., $\langle d_{\mathrm{NC}}\rangle_F = \langle d_{\mathrm{NC}}\rangle_0 + F/k$. However, the extracted Δx_0 are not entirely self-consistent. For example, Table 2 indicates that while $\Delta x_{0,\mathrm{I1-N}}$ is near zero, $\Delta x_{0,\mathrm{D-I1}}$ and $\Delta x_{0,\mathrm{D-N}}$ differs by 14 Å. If the value of $\Delta x_{0,\mathrm{D-I1}}$ is fixed to 33 Å to achieve self-consistency (since $\Delta x_{\mathrm{I1-N},0} \sim 0$), the quality of the fit is minimally affected (Figure 6, blue dotted line) and the agreement between the fitted $\Delta(1/k)_{\mathrm{D-I1}}$ and that estimated from Table 1 improves. This highlights the unreliability of fitting the D − I1 data to eq 1, which can be attributed to the following: (i) the narrow range of forces explored and (ii) the lack of data for forces close to 0 pN (i.e., 1−2 pN). Nevertheless, the reasonable agreement of the fitted parameters, Δx_0 and $\Delta(1/k)$, with that estimated from Table 1 indicates that eq 1 is a more accurate description of ΔG_F compared to the linear relation.

Although similar ΔG_0 were derived from both the linear fit and the fit to eq 1, the agreement is spurious as the forces being studied are close to 0 pN. The agreement is expected to be significantly poorer if there is a strong curvature in ΔG_F and if the range of forces explored is far from 0 pN.

TABLE 2: Parameters Extracted from Fitting ΔG_F to the Linear Relation, $\Delta G = \Delta G_0 - F\Delta x$, and to Equation 1, $\Delta G_F = \Delta G_0 - F\Delta x_0 + F^2\Delta(1/k)/2$[a]

states	linear	eq 1
I1−N	$\Delta G_0 = -1.06$ $\Delta x = 15.2$	$\Delta G_0 = -1.63$ $\Delta x_0 = 7.08 \times 10^{-7}$ $\Delta(1/k) = -3.80$
D − N	$\Delta G_0 = 8.1$ $\Delta x = 96.3$	$\Delta G_0 = 5.19$ $\Delta x_0 = 33.0$ $\Delta(1/k) = -13.9$
D−I1	$\Delta G_0 = 8.93$ $\Delta x = 79.0$	$\Delta G_0 = 7.45$ $\Delta x_0 = 46.5$ $\Delta(1/k) = -7.04$
D−I1		$\Delta G_0 = 6.81$ $\Delta x_0 = 33.0$ (fixed) $\Delta(1/k) = -10.03$

[a] $\Delta G(0)$ is in $k_{\mathrm{B}}T$, Δx_0 is in angstroms, and $\Delta(1/k)$ is in angsroms per piconewton.

Discussion

We have characterized, for the first time, the equilibrium properties of a protein (ddFLN4) in the presence of mechanical load using the tool of atomistic simulation. This in turn, allowed us to make a direct comparison of the states populated in the absence of a force and those populated as small forces (1−6 pN) are applied to pull the protein.

The equilibrium free-energy landscapes of ddFLN4 (SEKN and FEP, Figure 4) shows subtle shifts as the force is increased (0−6 pN). Upon the application of a force, we observe the

appearance of states that were hidden (i.e., negligibly populated and/or overlapping with other states) in the absence of the force. This suggests that even a small residual load on a protein (e.g., 2−3 pN) can alter the properties of the protein in the absence of force. Therefore, the free-energy landscape in the presence of a small force may not be directly related to that in the absence of a force and the details (e.g., nature of the intermediates) of the landscape could be force specific. The present results also demonstrate that it is difficult to establish a precise relationship between the intermediates seen in nonequilibrium unfolding pathways and the equilibrium landscape both in the absence and presence of a force. Furthermore, the mechanical response of a protein is anisotropic and depends on the pulling direction.[1,2] It is likely that the nature of the intermediates stabilized by the presence of the applied force will change as the pulling direction is changed.

If we disregard the case where the protein is two-state under *all* conditions, one consequence of the present results is that the kinetic mechanism derived from a bulk refolding study will not necessarily be the same as that derived from a mechanical refolding study. The model used here suggests that ddFLN4 is likely to be two-state in the absence of a force and three-state, as observed experimentally,[5,6,12] in the small interval of a forces (2−6 pN) studied here.

The relative free-energies of more extended states relative to N increase with the force in an approximately linear way as commonly assumed. While Δx gives a good indication of the "proximity" of a particular state to N, it is not the same as the difference in $\langle d_{NC} \rangle$ between pairs of states at zero force. The interpretation of Δx as a geometrical property of a single entity[16] is probably misguided. In principle, for free-energy minima or barriers with finite curvatures, a curvature in the plot of ΔG_F against the applied force is expected to be observed. If the $\langle d_{NC} \rangle$ is governed by a one-dimensional harmonic potential with a force independent spring constant, then the variation of ΔG_F can be described by eq 1.[19] Therefore, the linear relationship, $\Delta G_F = \Delta G_0 - F\Delta x$, is only valid when the relative extension between pairs of states is constant (i.e., force independent) or when the applied force is small enough such that $F^2 \sim 0$. Otherwise, the extracted Δx need not be the difference in $\langle d_{NC} \rangle$ between pairs of states as typically assumed. In addition, given the curvature of ΔG_F, estimates of ΔG_0 derived from a linear fit can deviate quite significantly from the true value especially when the range of forces probed is far from 0 pN. Our data can be fitted with an additional F^2 term (Figure 6) and is more accurately described by eq 1 than the linear relation. To this end, the extracted parameters (Δx_0 and $\Delta(1/k)$) are consistent with those independently derived from Table 1. However, for the D − I1 data at least, the range of forces explored is narrow and do not allow for a truly reliable fitting of the quadratic dependence on the force of the various free-energy differences.

The above results highlight the fact that while one-dimensional models are more easily implemented and sometimes unavoidable in practice, they tend to also mask the complexities of the system. That the FEPs along the "natural coordinate" and the utilization of d_{NC} or the rmsd as reaction coordinates obscure the number of intermediate states and/or the presence of multiple parallel pathways, which are evident from the SEKNs, clearly illustrates this point. We note that the free-energy is dependent on the definition of the reaction coordinate. If the reaction coordinate is poorly chosen, the free-energy of a "state", defined by a particular value of such a coordinate, will in actuality be the free-energy of a mixture of overlapping conformations each of which, may in reality be separated by sizable barriers (i.e., $> 1k_BT$). In this regard, the use of d_{NC} as a reaction coordinate for the interpretation of constant force experiments should be exercised with caution since it may not be able to discriminate between states, leading to an underestimate of kinetic barriers (e.g., see Figure 3a). Our results suggest that this may be particularly relevant for experiments that probe processes that occur at small forces (e.g., protein refolding) or involve transient, partially folded intermediates.

To conclude, our results indicate that the free-energy landscape of a protein under a small force is multidimensional and cannot be represented as a one-dimensional projection on a coordinate such as the extension. In addition, the effect of a force on the relative free-energy between a pair of states is more complex than the addition of a term proportional to the applied force (i.e., $-F\Delta x$) to the unperturbed free-energy difference. The force, even one as small as 2 pN, can significantly alter the nature of the equilibrium free-energy landscape. Thus, unless care has been taken to remove any residual load on the protein and not to overinterpret the states, especially when defined solely by d_{NC}, the properties (e.g., kinetics and mechanism of folding and unfolding) of a protein under mechanical load need not be straightforwardly related to that in the absence of a force.

Methods

All simulations were performed using the structure-based native-centric model of Karanicolas and Brooks,[22] where the protein is represented by a C_α trace and only native interactions are attractive. The topology and force-field parameters were generated using the lowest energy NMR structure of ddFLN4 (PDB no. 1ksr) after a steepest-descent energy minimization using an all-atom model with the EEF1 implicit solvent.[23] Langevin dynamics with a friction coefficient of 1 ps^{-1}, a time step of 15 fs, and holonomic constraints on all bonds was used.

When analyzing the simulations, native contacts were defined using a 9 Å cutoff and were only considered for pairs of residues at least four residues apart in the primary sequence. $\langle d_{NC} \rangle_F$ is defined as the distance between the N and C termini averaged over all conformers belonging to a particular state at force F.

The equilibrium kinetic network (EKN) was obtained by clustering long equilibrium MD trajectories in the principal component space defined by the distance between all atom pairs. The trajectories were projected onto the first three principal components and clustered into cubes of equal size where the size of the cubes were chosen such that there were 10000 clusters in total.

The cut-based free-energy profile (FEP) provide a complete description of the system kinetics by allowing one to compute the diffusion coefficient together with the free energy profile.[21] The FEPs were computed with the "pfoldf" procedure[24] and plotted along the natural coordinate for which the diffusive coefficient is constant and equal to one.[21] The trajectory saving interval was chosen to be 500 MD steps (75 ps) for the analysis of the dynamics to be in the diffusive regime as confirmed by comparing the FEPs for different saving intervals.

The simplified equilibrium kinetic network (SEKN), which describes inter basin kinetics, was constructed by iteratively partitioning the network into basins. The free-energy profile of the whole network was first built; if the resulting profile showed notable barriers, the profile was split into smaller basins. For this, we identified two representative nodes on each side of the barrier and divide the network by computing the "minimum cut" between nodes. The procedure was iteratively applied until all basins had no notable internal barriers. The number of effective transitions between each

pair of directly connected basins was then computed by assuming diffusive dynamics and using Kramers' equation to estimate the mean first passage time from one basin to the other.[21]

Abbreviations. MD, molecular dynamics; EKN, equilibrium kinetic network; SEKN, simplified equilibrium kinetic network; FEP, cut-based free-energy profiles; rmsd, root-mean-square deviation.

Acknowledgment. We acknowledge the Wellcome Trust and the University of Leeds for a studentship awarded to Z.T.Y. and Lucy Allen for discussions. We thank an anonymous referee for insightful comments and the suggestion to analyze the free-energies using the data in Table 1 as input by assuming that the extension is governed by a one-dimensional harmonic potential.

References and Notes

(1) Brockwell, D. J.; Paci, E.; Zinober, R. C.; Beddard, G. S.; Olmsted, P. D.; Smith, D. A.; Perham, R. N.; Radford, S. E. Pulling geometry defines the mechanical resistance of a β-sheet protein. *Nat. Struct. Biol.* **2003**, *10*, 731–737.

(2) Carrion-Vazquez, M.; Li, H.; Lu, H.; Marszalek, P. E.; Oberhauser, A. F.; Fernandez, J. M. The mechanical stability of ubiquitin is linkage dependent. *Nat. Struct. Biol.* **2003**, *10*, 738–743.

(3) Dietz, H.; Rief, M. Protein structure by mechanical triangulation. *Proc. Natl. Acad. Sci. USA* **2006**, *103*, 1244–1247.

(4) Carrion-Vasquez, M.; Marszalek, P. E.; Oberhauser, A. F.; Fernandez, J. M. Atomic force microscopy captures length phenotypes in single proteins. *Proc. Natl. Acad. Sci. USA* **1999**, *96*, 11288–11292.

(5) Schwaiger, I.; Schleicher, M.; Noegel, A. A.; Rief, M. The folding pathway of a fast-folding immunoglobulin domain revealed by single-molecule mechanical experiments. *EMBO Rep.* **2005**, *6*, 46–51.

(6) Schwaiger, I.; Kardinal, A.; Schleicher, M.; Noegel, A. A.; Rief, M. A mechanical unfolding intermediate in an Actin-crosslinking protein. *Nature Struct. Mol. Biol.* **2004**, *11*, 81–85.

(7) Cecconi, C.; Shank, E. A.; Bustamante, C.; Marqusee, S. Direct observation of the three-state folding of a single protein molecule. *Science* **2005**, *309*, 2057–2060.

(8) Ritort, F.; Bustamante, C.; Tinoco, I. A two-state kinetic model for the unfolding of single molecules by mechanical force. *Proc. Natl. Acad. Sci. USA* **2002**, *99*, 13544–13548.

(9) Brujic, J.; Hermans, R. I.; Walther, K. A.; Fernandez, J. M. Single-molecule force spectroscopy reveals signatures of glassy dynamics in the energy landscape of ubiquitin. *Nat. Phys.* **2006**, *2*, 282–286.

(10) Dudko, O. K.; Hummer, G.; Szabo, A. Intrinsic rates and activation free energies from single-molecule pulling experiments. *Phys. Rev. Lett.* **2006**, *96*, 108101.

(11) Schlierf, M.; Rief, M. Single-molecule unfolding force distributions reveal a funnel-shaped energy landscape. *Biophys. J.* **2006**, *90*, L33−L35.

(12) Schlierf, M.; Berkemeier, F.; Rief, M. Direct observation of active protein folding using lock-in force spectroscopy. *Biophys. J.* **2007**, *93*, 3989–3998.

(13) Dietz, H.; Rief, M. Exploring the energy landscape of GFP by single-molecule mechanical experiments. *Proc. Natl. Acad. Sci. USA* **2004**, *101*, 16192–16197.

(14) Peng, Q.; Li, H. Atomic force microscopy reveals parallel mechanical unfolding pathways of T4 lysozyme: evidence for a kinetic partitioning mechanism. *Proc. Natl. Acad. Sci. USA* **2008**, *105*, 1885–1890.

(15) Sandal, M.; Valle, F.; Tessari, I.; Mammi, S.; Bergantino, E.; Musiani, F.; Brucale, M.; Bubacco, L.; Samori, B. Conformational equilibria in monomeric alpha-synuclein at the single-molecule level. *PLoS Biol.* **2008**, *6*, e6.

(16) Dougan, L.; Feng, G.; Lu, H.; Fernandez, J. M. Solvent molecules bridge the mechanical unfolding transition state of a protein. *Proc. Natl. Acad. Sci. USA* **2008**, *105*, 3185–3190.

(17) Oberhauser, A. F.; Marszalek, P. E.; Erickson, H. P.; Fernandez, J. M. The molecular elasticity of extracellular matrix protein tenascin. *Nature* **1998**, *393*, 181–185.

(18) Schlierf, M.; Rief, M. Temperature softening of a protein in single-molecule experiments. *J. Mol. Biol.* **2005**, *354*, 497–503.

(19) Sachs, F.; Lecar, H. Stochastic models for mechanical transduction. *Biophys. J.* **1991**, *59*, 1143–1145.

(20) Krivov, S. V.; Karplus, M. Hidden complexity of free energy surfaces for peptide (protein) folding. *Proc. Natl. Acad. Sci. USA* **2004**, *101*, 14766–14770.

(21) Krivov, S. V.; Karplus, M. Diffusive reaction dynamics on invariant free energy profiles. *Proc. Natl. Acad. Sci. USA* **2008**, In press.

(22) Karanicolas, J.; Brooks., C. L. I. The structural basis for biphasic kinetics in the folding of the WW domain from a formin-binding protein: Lessons for protein design. *Proc. Natl. Acad. Sci. USA* **2003**, *100*, 3954–3959.

(23) Lazaridis, T.; Karplus, M. Effective energy function for protein dynamics and thermodynamics. *Proteins* **1999**, *35*, 133–152.

(24) Krivov, S. V.; Karplus, M. One-dimensional free-energy profiles of complex systems: Progress variables that preserve the barriers. *J. Phys. Chem. B* **2006**, *110*, 12689–12698.

JP807316E